P−*V*−*T*−*x* and VLE Properties of Difluoromethane (R32) + 1,1,1,2,3,3-Hexafluoropropane (R236ea) and Pentafluoroethane (R125) + R236ea Systems Derived from Isochoric Measurements

Giovanni Di Nicola* and Fabio Polonara

Dipartimento di Energetica, Università di Ancona, 60100 Ancona, Italy

Roman Stryjek

Institute of Physical Chemistry, Polish Academy of Sciences, 01-224 Warsaw, Poland

Isochoric *P*−*V*−*T*−*x* measurements were performed for the difluoromethane (R32) + 1,1,1,2,3,3-hexafluoropropane (R236ea) and pentafluoroethane (R125) + 1,1,1,2,3,3-hexafluoropropane (R236ea) systems within the 254−364 K temperature range and within the 111−1994 kPa pressure range. Measurements for the R32 + R236ea system were taken for 6 different compositions and 10 expansion series, resulting in 188 data points, 101 of which were within the VLE boundary and 87 of which were in the superheated vapor region. Measurements for the R125 + R236ea system were taken for 4 different compositions and 10 expansion series, for a total of 213 data points, 133 of which were within the VLE boundary and 80 of which were in the superheated vapor region. In all, 346 data points are presented. The VLE parameters were derived from experimental data using a flash method and the Carnahan−Starling−De Santis equation of state (CSD EOS). The dew point parameters were obtained by the interpolation of the *P*−*T* isochoric sequence. Data from the superheated vapor region were interpreted using tried and tested correlation methods for the second and third virial coefficients. The results, both within the VLE boundary and in the superheated region, revealed a mutual consistency close to the experimental uncertainty that we evaluated.

Introduction

In the search for fluids for potential applications as refrigerants in high-temperature heat pumps, centrifugal chillers, and chemical blowing agents, two new refrigerants, namely, 1,1,1,3,3,3-hexafluoropropane (R236fa) and 1,1,1,2,3,3-hexafluoropropane (R236ea), are among the most promising. Their properties differ, however, from those of 1,2-dichloro-1,1,2,2-tetrafluoroethane (R114), and other fluids with more suitable properties are likely to be found among the mixtures, be they azeotropic or zeotropic. Data in the literature and our previous measurements[1] show that binary mixtures of R236fa with other fluoroderivatives show a limited deviation from Raoult's law, whereas binary mixtures formed by R236fa with hydrocarbons (propane, *i*-butane) show strong positive deviations from Raoult's law, with the formation of azeotropes. A similar behavior can be observed for the systems with R236ea, also in view of its higher dipole moment. Even if the VLE and *P*−*V*−*T*−*x* behavior of refrigerants can be roughly estimated, the availability of experimental data makes it possible to optimize the properties of working fluids by adjusting the composition of the mixture. In addition, the VLE and *P*−*V*−*T*−*x* properties should make up for any severe deficiency in the basic thermodynamic properties of a new group of mixtures comprising fluoroderivatives of propane. Following our previous studies on refrigerant properties using the isochoric method,[1−3] we report here our findings for two binary systems containing R236ea.

The experimental results cover a temperature range from 254 to 364 K and a pressure range from 111 to 1994 kPa. In addition, both the *P*−*V*−*T*−*x* and the VLE regions are covered. Experimental VLE data from Bobbo et al.[4] were measured at temperatures of 288, 303, and 318 K. To our knowledge, the *P*−*V*−*T*−*x* data for the selected binaries have not been reported elsewhere in the literature.

Experimental Section

Reagents. R32 (CAS Reg. No. 75-10-5) and R125 (CAS Reg. No. 354-33-6) were donated by Ausimont Spa of Italy, and R236ea (CAS Reg. No. 431-63-0) was supplied by Lancaster Synthesis, Inc. Their purities were checked by the authors using gas chromatography: the purities of the R32 and R125 were better than 99.98%, while the purity of the R236ea was better than 99.99% in terms of peak area ratios.

Experimental Setup. The experimental work was carried out using the apparatus described elsewhere,[5] and a diagram of it was presented in a proceeding paper.[1] It was used as is, so only the essential details and the uncertainty for the quantities measured are given here. The main element in the setup is a constant-volume spherical cell with a total capacity of ($0.2548 \pm 3 \times 10^{-4}$) dm^3. The temperature was stabilized to within ±5 mK and was measured with uncertainties of ±15 mK for temperatures above 268 K and ±30 mK for temperatures below 268 K. Pressure was measured to within ±0.5 kPa. The experimental method is described in detail in Di Nicola et al.,[1,2]

* Corresponding author. Dipartimento di Energetica, Università di Ancona, via Brecce Bianche, 60100 Ancona, Italy. Tel.: +39-071-2204432. Fax: +39-071-2804239. E-mail: anfreddo@popcsi.unian.it.

10.1021/je000260w CCC: $20.00
Published on Web 02/17/2001

Table 1. Compositions of the Investigated Systems

sample	no. of exp. points total	VLE	vapor	m_1 (g)	m_2 (g)	x_1	Σn
			R32 (1) + R236ea (2)				
1	18	9	9	1.043	3.815	0.44419	0.0451
2	19	8	11	1.285	4.698	0.44419	0.0556
3	19	11	8	1.800	6.583	0.44419	0.0779
4	16	10	6	3.830	10.670	0.51200	0.1438
5	19	16	3	5.524	15.388	0.51200	0.2074
6	23	16	7	6.105	8.035	0.68952	0.1702
7	15	7	8	1.970	2.221	0.72169	0.0525
8	19	7	12	2.135	2.407	0.72169	0.0569
9	23	12	11	4.083	3.700	0.76332	0.1028
10	17	5	12	1.943	1.272	0.81707	0.0374
			R125 (1) + R236ea (2)				
1	22	11	11	2.175	4.917	0.35910	0.0505
2	22	14	8	3.192	7.218	0.35910	0.0741
3	23	17	6	4.177	9.443	0.35910	0.0969
4	20	9	11	3.008	3.218	0.54209	0.0462
5	18	9	9	3.688	3.946	0.54209	0.0567
6	20	12	8	4.161	4.452	0.54209	0.0640
7	23	14	9	6.627	4.682	0.64198	0.0860
8	23	15	8	10.160	7.178	0.64198	0.1319
9	22	19	3	15.086	10.658	0.64198	0.1958
10	20	13	7	8.825	5.215	0.68191	0.1078

including the part regarding the mixture's preparation by a gravimetric method. The uncertainty of the measured quantities were reported. The samples were charged from special bottles weighed on an analytical balance (uncertainty = ±0.3 mg). The same method was used for the partial discharging of the isochoric cell. The uncertainty in the mass of the first charge was estimated to be lower than ±1 mg, and it increased to ±1.2 mg after the partial expansions. The uncertainty for the mass after the first charge yields an uncertainty for the molar fraction that is consistently within $\pm 3.5 \times 10^{-5}$. Taking into account the uncertainty in the charged mass, the pressure range, and the uncertainty resulting from the calibration of the isochoric cell, we estimated the uncertainty in the calculated molar volume of superheated vapor to be consistently lower than $\pm 9 \times 10^{-2}$ dm^3 mol^{-1}. From the single uncertainties, the overall experimental uncertainty in terms of pressure, calculated using the laws of propagation, was estimated to be lower than ±0.6 kPa for measurements within the VLE boundary and lower than ±1.1 kPa in the superheated vapor region.

Results and Discussion

The basic information on the prepared mixtures is presented in Table 1, and the distribution of the $P-V-T-x$ measurements is shown in Figure 1. The experimental $P-T$ data collected for each isochore were plotted as pressure versus temperature, and each experimental point was assigned as being within the VLE boundary or pertaining to the superheated region. The results within the VLE boundary are presented in Tables 2 and 3 for the R32 + R236ea and R125 + R236ea systems, respectively. The results assigned to the superheated vapor region are shown in Tables 4 and 5 for the R32 + R236ea and R125 + R236ea systems, respectively. The molar volume, V, of superheated vapor was calculated from the equation

$$V = V_{iso}/n \tag{1}$$

where V_{iso} and n are the isochoric cell volume and the number of charged moles, respectively, and the values are included in Tables 4 and 5 and correlated with the experimental values.

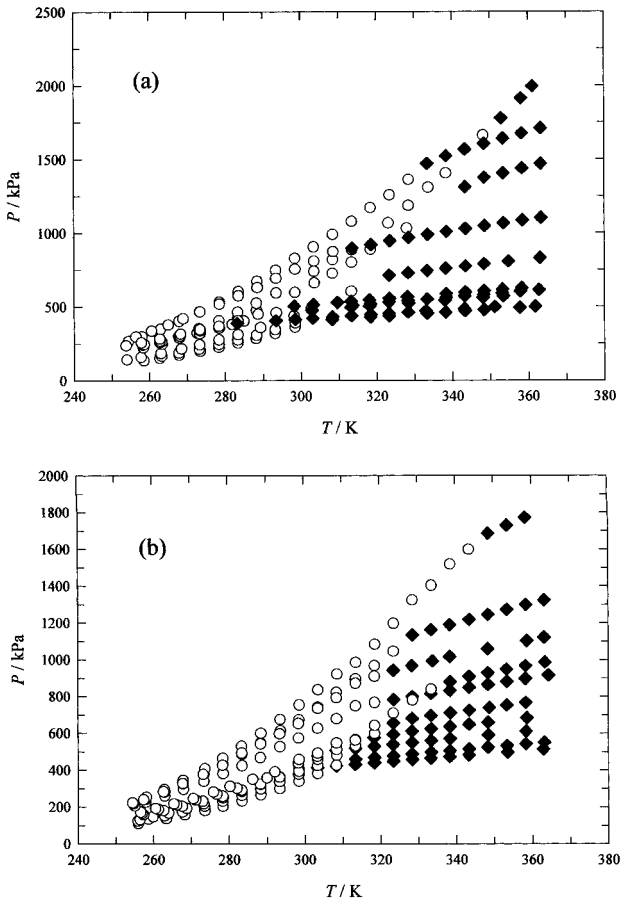

Figure 1. Distribution of the $P-V-T-x$ measurements for the systems (a) R32 + R236ea and (b) R125 + R236ea. ○, data within the VLE boundary; ◆, data in the superheated vapor region. Notation of series: ○, 1st; ●, 2nd; □, 3rd; ■, 4th; △, 5th; ▲, 6th; ▽, 7th; ▼, 8th; ◇, 9th; and ◆, 10th.

VLE Derivation. By applying the CSD EOS[6] in the form

$$\frac{PV}{RT} = \frac{1 + Y + Y^2 - Y^3}{(1 - Y)^3} - \frac{a}{RT(V + b)} \tag{2}$$

where

$$Y = \frac{b}{4V} \tag{3}$$

the VLE parameters were derived by means of two methods. In eq 2, R is the universal gas constant, P is the pressure, and T is the absolute temperature. In eq 2, parameters a and b are function of temperature; respective expressions and their coefficients, which are reported in Table 6 for the reader's convenience, were adapted from ref 7. For mixtures, a one-fluid model was applied with one adjustable parameter, $K_{ij} = K_{ji}$ for $i \neq j$, per binary system.

(a) The Flash Method. Each data point within the VLE boundary was correlated individually. The T, P, and z_i values were kept constant, and the value of the binary interaction parameter, K_{12}, was adjusted with the standard flash method,[8] considering the volume balance of both phases, as explained elsewhere.[2] The necessary molar volumes are obtained from the CSD EOS. The K_{12} values calculated in this way are presented graphically in Figures 2 and 3.

In addition, the composition and pressure at the bubble and dew points could be found for each data (T, P, z_i) set. Assuming that they are temperature-independent, we

Table 2. Experimental Data within the VLE Boundary for the R32 + R236ea System

sample	T (K)	P (kPa)	sample	T (K)	P (kPa)
1	258.45	136.4		338.32	1404.1
	262.68	152.4		348.19	1660.8
	267.83	173.9			
	273.36	199.0	6	254.38	266.0
	278.29	224.8		257.96	298.9
	283.28	253.4		262.86	348.0
	288.15	284.9		267.82	402.3
	293.17	319.6		273.18	465.6
	298.40	362.4		278.42	532.4
				283.50	602.4
2	263.18	166.9		288.43	671.5
	267.77	188.2		293.39	746.0
	273.14	214.2		298.43	827.5
	278.30	243.8		303.38	905.3
	283.28	274.3		308.39	989.1
	288.29	307.2		313.42	1077.9
	293.22	344.8		318.42	1170.5
	298.53	390.1		323.42	1256.6
				328.44	1360.8
3	253.97	142.1			
	257.72	159.0	7	258.13	242.3
	263.01	184.7		263.16	263.2
	268.41	215.3		267.84	289.7
	273.18	243.3		273.25	318.5
	278.38	276.7		278.40	355.9
	283.36	312.0		281.81	380.5
	289.32	358.0		284.98	402.2
	298.25	437.1		293.51	458.1
	302.71	481.6			
	313.28	603.3	8	258.52	245.1
				262.75	269.1
4	263.32	247.5		268.05	301.0
	272.55	322.6		273.41	336.6
	283.28	421.7		278.34	367.2
	288.25	476.4		283.38	405.5
	298.43	596.9		288.71	450.0
	303.58	660.9			
	308.33	724.4	9	256.38	297.6
	313.40	800.1		260.52	335.9
	318.37	888.3		264.92	378.2
	327.97	1031.0		268.89	419.3
				273.27	466.1
5	258.33	223.8		278.44	518.9
	262.71	257.8		283.47	573.7
	267.77	301.6		288.49	630.1
	273.05	351.7		293.41	692.3
	278.35	407.1		298.45	753.9
	283.27	463.2		303.44	808.0
	288.24	524.2		308.51	872.3
	293.45	593.1			
	303.43	739.2	10	253.75	236.8
	308.40	818.8		257.80	257.8
	313.45	885.0		262.69	281.9
	323.10	1066.5		268.19	316.0
	328.40	1184.5		273.29	345.4
	333.65	1307.8			

found the average values of $K_{12} = -0.05097$ and $K_{12} = -0.001737$ for the R32 + R236ea and R125 + R236ea systems, respectively. The graphs show that the K_{12} values are slightly temperature-dependent, however. Assuming a linear temperature dependence, we found $K_{12} = -0.4648 \times 10^{-2} - (1.62561 \times 10^{-4})(T/\mathrm{K} - 273.15)$ and $K_{12} = 0.062996 - (2.25331 \times 10^{-4})(T/\mathrm{K} - 273.15)$.

As a second step, the values of K_{12} found (with or without consideration of its temperature dependence) were used to reproduce all of the VLE data, with T and z_i held constant and pressure taken as the dependent variable. The pressure deviations calculated in this way for each isochore are given in Table 7, and the pressure deviations obtained when the temperature dependence of K_{ij} was considered are shown in Figures 4 and 5. However, it is evident from the results in Table 7 that the improvements induced in the data representation by implementing K_{12} as temperature-dependent are relatively small.

Table 3. Experimental Data within the VLE Boundary for the R125 + R236ea System

sample	T (K)	P (kPa)	sample	T (K)	P (kPa)
1	255.97	110.7		286.22	349.6
	263.37	137.1		292.10	390.2
	268.27	156.6		298.44	457.1
	273.54	179.8		303.37	491.2
	278.38	203.4		308.37	546.7
	283.42	232.5		313.30	561.5
	288.35	264.6			
	293.38	298.4	7	255.00	205.6
	298.42	338.9		258.02	225.3
	303.37	380.6		262.92	259.2
	308.32	426.6		267.88	295.7
				273.30	337.9
2	255.84	122.3		278.40	379.6
	258.68	133.5		283.39	423.2
	262.97	151.6		288.26	467.2
	267.65	173.3		293.42	525.9
	273.45	203.0		298.34	572.1
	278.28	230.7		303.35	626.5
	283.33	263.1		308.35	677.0
	288.31	297.1		313.33	748.4
	293.34	336.8		318.36	765.8
	298.36	376.9			
	303.38	423.5	8	254.64	216.5
	308.42	479.8		258.01	241.9
	313.31	532.0		262.91	281.8
	318.35	597.9		267.80	325.2
				273.28	378.3
3	256.39	131.8		278.33	430.5
	259.88	147.1		283.37	485.8
	263.96	166.6		288.33	545.6
	268.75	191.5		293.54	612.3
	273.31	217.5		298.39	672.0
	278.36	248.7		303.40	740.1
	283.31	283.6		308.34	821.3
	288.33	321.1		313.40	893.9
	293.37	361.4		318.40	966.9
	298.39	407.2		323.38	1044.6
	303.36	457.6			
	308.36	510.5	9	254.46	222.5
	313.37	564.8		258.06	252.3
	318.35	641.0		262.86	295.1
	323.33	708.2		267.80	343.9
	328.35	779.2		273.56	407.0
	333.32	838.5		278.28	463.2
				283.27	527.6
4	257.38	157.9		288.36	599.2
	262.67	180.7		293.43	673.8
	267.56	202.7		298.50	753.0
	273.03	230.4		303.46	835.6
	278.28	257.7		308.48	921.4
	283.28	290.3		313.47	984.3
	288.26	323.2		318.46	1082.7
	293.31	361.7		323.40	1196.4
	298.40	391.7		328.36	1323.6
				333.38	1401.9
5	256.96	164.7		338.38	1516.8
	261.20	186.9		343.32	1597.5
	266.10	210.9			
	271.15	237.2	10	257.33	239.2
	276.72	269.0		262.61	282.2
	282.03	301.3		267.72	326.8
	289.98	356.6		273.10	376.9
	298.29	436.7		278.24	426.7
	303.30	473.8		283.34	491.8
				288.29	541.4
6	256.57	171.9		293.34	595.5
	260.55	191.9		298.29	651.8
	265.35	217.0		303.40	734.9
	270.48	245.7		308.33	791.2
	275.82	281.0		313.32	870.3
	280.18	310.3		318.32	908.6

Table 4. Experimental Data in the Superheated Vapor Region for the R32 + R236ea System

sample	T (K)	P (kPa)	V (dm^3 mol^{-1})	sample	T (K)	P (kPa)	V (dm^3 mol^{-1})
1	308.24	413.2	5.647		363.28	1709.7	1.502
	318.38	430.1	5.649				
	323.28	438.1	5.651	7	302.92	476.4	4.857
	333.35	454.3	5.653		313.29	496.2	4.859
	338.14	462.0	5.655		318.12	505.3	4.860
	343.34	470.3	5.656		328.38	524.5	4.862
	348.32	478.4	5.657		338.02	542.5	4.864
	357.70	492.6	5.660		348.05	560.7	4.867
	361.80	500.6	5.659		353.41	570.6	4.868
2	313.69	509.3	4.586	8	298.22	504.0	4.480
	318.37	519.6	4.587		303.28	514.7	4.481
	323.24	529.7	4.589		309.61	527.9	4.482
	328.26	540.0	4.590		313.23	535.5	4.483
	333.28	550.3	4.591		318.11	544.5	4.484
	338.33	560.5	4.592		323.35	556.3	4.485
	343.20	570.3	4.593		328.09	566.0	4.486
	348.23	580.5	4.594		338.33	586.8	4.488
	353.09	590.3	4.599		343.32	596.7	4.490
	357.90	603.2	4.596		348.29	606.7	4.491
	362.76	614.0	4.597		353.17	616.6	4.492
					358.23	626.8	4.493
3	323.28	713.3	3.275				
	328.31	729.2	3.276	9	313.51	897.0	2.480
	333.32	744.2	3.276		318.50	921.1	2.481
	338.25	758.9	3.277		323.49	946.7	2.481
	343.40	774.2	3.278		328.45	969.2	2.482
	348.33	788.9	3.279		333.43	989.0	2.482
	354.76	807.4	3.280		338.40	1008.5	2.483
	363.07	830.1	3.281		343.42	1027.9	2.484
					348.44	1047.1	2.484
4	338.29[a]	1222.0	1.775		353.45	1066.2	2.485
	343.37	1311.4	1.776		358.44	1085.1	2.485
	348.40	1374.9	1.776		363.31	1101.5	2.486
	353.38	1404.5	1.777				
	358.37	1438.4	1.777	10	283.17	389.1	5.570
	363.26	1468.2	1.777		293.42	406.1	5.573
					298.51	414.6	5.574
5	352.85	1777.7	1.232		303.13	422.1	5.575
	358.12	1913.3	1.232		308.37	431.0	5.577
	361.12	1993.8	1.232		313.37	438.7	5.578
					318.45	447.0	5.579
6	333.35	1470.6	1.500		323.24	454.6	5.580
	338.35	1522.0	1.500		328.31	462.7	5.582
	343.34	1566.3	1.500		332.97	470.1	5.583
	348.38	1604.8	1.501		343.10	486.0	5.586
	353.36	1640.2	1.501		351.07	498.5	5.588
	358.29	1675.0	1.501				

[a] Denotes experimental points that were not considered in the final data reduction.

(b) The Interpolation Method. The dew point parameters were found by interpolating data from the superheated vapor and the two-phase regions. A discontinuity in $(\partial P/\partial T)_{V,z_i}$ coincides with the dew point. To find the dew point (P, T, y_i) parameters numerically, the data above and below the dew point were fitted separately. The data within the VLE boundary were regressed using the Antoine type of equation. We observed a random distribution of the deviations plotted versus temperature, and because they were independent of the charged mass and composition, they correspond mainly to the random error in equilibrium measurements. The data in the superheated vapor region were fitted to a second-degree polynomial. The two equations were then solved simultaneously for pressure and temperature, and the solution was adopted as the dew point. After the dew point was established, the CSD EOS was used, thereby enabling K_{12} and x_i to be determined. In this way, we found the mean values $\bar{K}_{12} = -0.0419$ and $\bar{K}_{12} = -0.0277$ for the R32 + R236ea and R125 + R236ea systems, respectively. The results are given in Table 8.

Table 5. Experimental Data in the Superheated Vapor Region for the R125 + R236ea System

sample	T (K)	P (kPa)	V (dm^3 mol^{-1})	sample	T (K)	P (kPa)	V (dm^3 mol^{-1})
1	313.38	458.6	5.053		333.27	560.4	4.503
	318.37	468.2	5.054		338.29	570.8	4.504
	323.33	477.6	5.055		348.38	591.4	4.506
	328.31	487.0	5.057		358.31	611.6	4.508
	333.33	496.4	5.058				
	338.27	505.5	5.059	6	318.23	577.5	3.988
	343.34	514.9	5.060		323.31	594.4	3.989
	348.30	524.0	5.061		328.24	611.4	3.990
	353.32	533.1	5.063		333.31	624.4	3.991
	358.28	542.2	5.064		338.30	636.2	3.992
	363.15	551.0	5.065		343.34	648.1	3.993
					348.32	659.8	3.994
2	323.32[a]	655.0	3.444		358.53	683.6	3.996
	328.30	681.1	3.445				
	333.26	695.7	3.446	7	323.39	782.8	2.966
	338.37	710.6	3.447		328.32	799.4	2.967
	343.37	724.9	3.447		333.26	815.8	2.968
	348.63	739.9	3.448		338.26	832.3	2.968
	353.23	752.8	3.449		343.34	849.0	2.969
	358.24	767.1	3.450		348.26	865.0	2.970
					353.29	881.3	2.970
3	338.33[a]	879.9	2.634		358.16	897.0	2.971
	343.33	908.6	2.635		364.22	916.4	2.972
	348.30	928.8	2.636				
	353.20	947.9	2.636	8	328.40	1134.8	1.935
	358.20	967.2	2.637		333.31	1162.4	1.936
	363.34	986.9	2.638		338.24	1189.7	1.936
					343.38	1218.0	1.936
4	303.32[a]	413.8	5.514		348.31	1244.7	1.937
	308.31	422.6	5.515		353.34	1271.7	1.937
	313.30	431.2	5.516		358.29	1298.0	1.938
	318.29	439.6	5.517		363.16	1323.7	1.938
	323.34	448.1	5.519				
	328.35	456.6	5.520	9	348.41[a]	1685.6	1.305
	333.23	464.9	5.521		353.37	1729.4	1.305
	338.19	473.1	5.523		358.18	1771.3	1.305
	343.28	481.5	5.524				
	353.47	496.9	5.527	10	323.36	943.3	2.366
	362.91	513.3	5.529		328.23	967.9	2.366
					333.68	992.9	2.367
5	308.18[a]	507.2	4.498		338.22	1016.7	2.368
	313.31	518.1	4.499		348.21	1059.2	2.369
	318.31	528.7	4.500		358.54	1102.7	2.370
	323.25	539.2	4.501		363.13	1121.4	2.370
	328.31	550.1	4.502				

[a] Denotes experimental points that were not considered in the final data reduction.

When the K_{12} values obtained with the two methods were compared, we found that they produce some differences in the system pressure. Here, for the comparison, K_{12} values were calculated on the basis of the temperature dependence. Our results were also compared with those found by Bobbo et al.[4] for their experimental VLE data at 288.54, 303.19, and 318.24 K. The respective values calculated at $x = 0.5$, where the deviation reaches its maximum value, are shown in Table 9. Even if these differences are systematic, they are within the upper limit of our experimental errors. The magnitude of the differences is justified by the fact that our data come from indirect methods. In addition, our data carry some uncertainty resulting from the volumetric property representation used by the model in the saturation range and the empirical nature of the equations used for the data interpolation to the dew point. An analysis of K_{12} plotted versus temperature also revealed a slight but clearly evident temperature dependence. The data displayed a steeper slope at higher temperatures. This behavior is even more evident at temperatures above the critical temperature of the lower-boiling components and has a characteristic shape for all of the systems studied

Table 6. a_i and b_i Coefficients of the CSD EOS and Parameters for R32, R125, and R236ea

		compound	
parameter	R32	R125	R236ea
a_0 (kPa dm^6 mol^{-2})	1662.2699	3427.9219	5611.9106
a_1 (K^{-1})	$-2.1975227 \times 10^{-3}$	$-3.1746132 \times 10^{-3}$	$-2.4948509 \times 10^{-3}$
a_2 (K^{-2})	-1.889027×10^{-6}	$-1.7572861 \times 10^{-6}$	$-1.7370031 \times 10^{-6}$
b_0 (dm^3 mol^{-1})	0.077987924	0.14938043	0.19314696
b_1 (dm^3 mol^{-1} K^{-1})	$-0.75238102 \times 10^{-4}$	$-1.8085107 \times 10^{-4}$	$-1.8123708 \times 10^{-4}$
b_2 (dm^3 mol^{-1} K^{-2})	$-0.5301071 \times 10^{-7}$	$-1.1881331 \times 10^{-7}$	$-1.3230688 \times 10^{-7}$
T_c (K)	351.26	339.33	412.44
P_c (kPa)	5782	3629	3502
V_c (dm^3 mol^{-1})	0.12269	0.210082	0.27005
ω	0.276904	0.303667	0.3794
μ (debye)	1.978	1.563	1.129

Table 7. Deviations in Pressure, as ΔP (%), from the Fit of the Data within the VLE Boundary: (a) Disregarding the Temperature Dependence of K_{12} and (b) Considering a Linear Temperature Dependence of K_{12}

sample	a		b		sample	a		b	
R32 + R236ea	bias	AAD	bias	AAD	R125 + R236ea	bias	AAD	bias	AAD
1	0.02	0.16	−0.27	0.37	1	0.24	0.62	−0.17	0.38
2	0.1	0.24	−0.11	0.25	2	0.84	0.97	0.34	0.58
3	0.73	0.73	0.29	0.73	3	0.62	1.16	0.29	0.67
4	0.48	0.94	0.66	0.97	4	0.75	0.78	0.11	0.34
5	0.67	1.39	0.82	1.01	5	0.09	0.85	−0.69	1.00
6	0.31	1.34	0.30	0.89	6	0.47	1.5	−0.02	0.7
7	−0.01	1.00	−0.38	1.08	7	0.16	0.92	−0.34	0.52
8	−0.49	0.63	−0.87	0.87	8	0.55	1.08	0.38	0.75
9	0.32	0.83	0.15	0.43	9	−0.13	1.56	−0.02	1.08
10	−0.46	0.58	−1.04	1.04	10	−0.14	0.69	−0.38	1.16
average	0.27	0.88	0.12	0.77	average	0.34	1.06	0.00	0.74

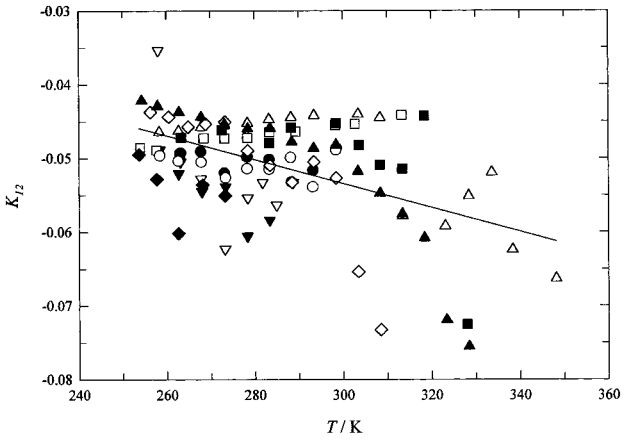

Figure 2. Scatter diagram of K_{12} values versus temperature for the R32 + R236ea system. The line represents the linear temperature dependence of K_{12}.

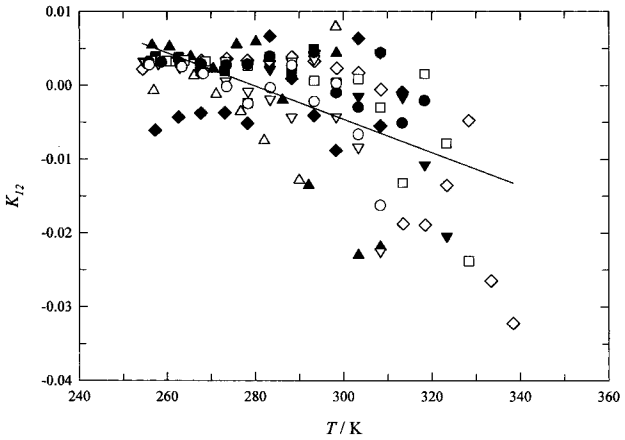

Figure 3. Scatter diagram of K_{12} values versus temperature for the R125a + R236ea system. The line represents the linear temperature dependence of K_{12}.

here and for the recently presented results. This might be due either to greater difficulties in approaching equilibrium in this temperature range or to an insufficiently accurate representation of the fluid property by the CSD EOS, for which the coefficients were found from the fit of saturated properties.

Considering the bubble point behavior, both systems are zeotropic with negative deviations from Raoult's Law.

***P*−*V*−*T*−*x* Modeling.** Experimental data in the superheated vapor region within the reduced temperature ranges of 0.89−0.98 for the R32 + R236ea system and 0.86−1.03 for the R125 + R236ea system were interpreted by means of the virial EOS. Expressed in terms of the inverse molar volume, the virial EOS takes the following form if it is truncated after the third term:

$$P = \frac{RT}{V}\left(1 + \frac{B}{V} + \frac{C}{V^2}\right) \tag{4}$$

where B and C are the second and third virial coefficients, respectively. Based on the considerations that our isochoric experimental method does not allow points to be retrieved along isotherms and that the pressure and temperature ranges of our data are relatively limited, we chose to compare our experimental pressure and molar volume data with the correlating methods available in the literature. From among the more general correlations describing second virial coefficients, we used the one proposed by Tsonopoulos,[8,9] while for the third virial coefficients, we used the correlation proposed by Orbey and Vera.[10] In each method appears only one adjustable parameter, L_{ij}, per binary system, which describes the cross-critical temperature

$$T_{ij}^c = (T_i^c\, T_j^c)^{1/2}(1 - L_{ij}) \tag{5}$$

and is needed to describe the course of the critical temperature of the mixtures. For a two-component system, L_{ij}

Table 8. Dew Point Parameters for the Studied Systems[a]

sample	T (K)	P (kPa)	K_{12}	x_1	sample	T (K)	P (kPa)	K_{12}	x_1
		R32 + R236ea					R125 + R236ea		
1	303.49	405.6	−0.0538	0.13228	1	311.00	454.1	−0.0190	0.11739
2	310.48	503.9	−0.0647	0.14824	2	323.23	658.0	−0.0160	0.13086
3	322.00	709.2	−0.0726	0.16926	3	333.19	854.3	−0.0344	0.15398
4	330.02	1069.6	0.0070	0.18128	4	299.19	406.7	−0.0050	0.18598
5	340.77	1461.9	0.0266	0.19672	5	307.81	506.3	−0.0478	0.23539
6	335.11	1494.0	−0.0859	0.39688	6	309.01	547.0	−0.0224	0.21931
7	288.87	449.2	0.0026	0.24167	7	316.12	758.4	−0.0529	0.33454
8	294.74	496.8	−0.0597	0.31128	8	328.76	1136.8	−0.0296	0.35551
9	308.72	874.5	−0.0568	0.39746	9	344.70	1653.1	−0.0505	0.40578
10	280.46	384.6	−0.0611	0.38959	10	315.67	896.4	0.0004	0.34529
average			−0.0419		average			−0.0277	

[a] T and P found by interpolation, K_{12} and x_1 found from the CSD EOS.

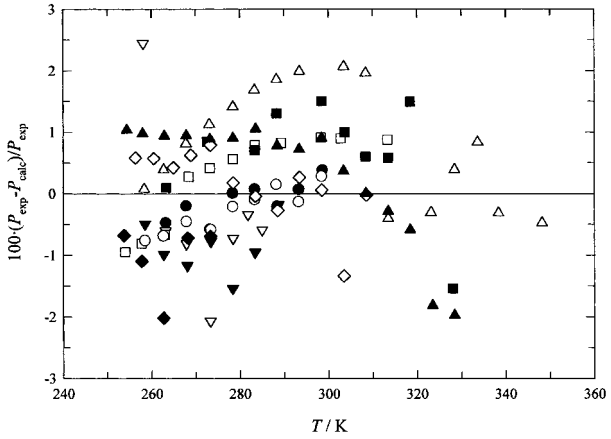

Figure 4. Deviations in pressure versus temperature calculated considering the temperature dependence of K_{12} for the R32 + R236ea system.

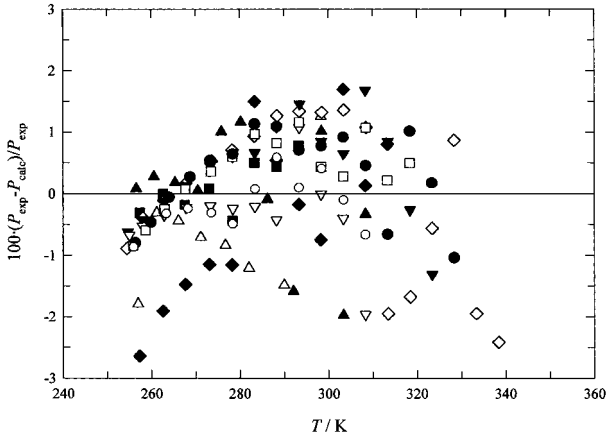

Figure 5. Deviations in pressure versus temperature calculated considering the temperature dependence of K_{12} for the R125 + R236ea system.

$= 0$ and $L_{ij} = L_{ji}$. The parameters used were adopted from ref 12 and are included in Table 6. The value of the binary interaction parameter (L_{ij}) needed to calculate the critical temperature of the mixtures was not available in the literature. To overcome this problem, we used several different L_{ij} values and observed that the differences in the results were small over quite a wide range of the attempted values; we ultimately adopted $L_{12} = 0.025$ for the binary systems.

Considering the volumetric properties, eq 4 was rewritten as

$$(PV/RT - 1)V = B + \frac{C}{V} \tag{6}$$

Table 9. Calculated Deviations in Pressure at $x_1 = 0.5$ for the Studied Systems

		K_{12}[a]		
system	T (K)	this work	ref 4	dP[b] (%)
R32 + R236ea	288.54	−0.05085	−0.04351	0.99
	303.19	−0.05638	−0.04130	1.91
	318.24	−0.06207	−0.03933	2.71
R125 + R236ea	288.54	−0.00202	0.00559	1.10
	303.19	−0.00532	0.00540	1.46
	318.24	−0.00871	0.00629	1.94

[a] K_{12} calculated with flash method. [b] $dP = 100(P_{lit} - P_{our})/P_{lit}$.

The deviation in molar volume was calculated for each ith point, using experimental P, T, V, and x values, as follows:

$$\Delta V = [PV/(RT) - 1]V - (B + C/V) \tag{7}$$

in which B and C are calculated by the Tsonopoulos[9,10] and Orbey and Vera[11] methods, respectively. The absolute average deviation (AAD) and bias in volume were calculated as

$$\text{AAD} = \sum_{i=1}^{N} \text{abs}(\Delta V_i)/N \tag{8}$$

and

$$\text{bias} = \sum_{i=1}^{N} \Delta V_i/N \tag{9}$$

where N stands for the number of experimental points.

In a similar way, we calculated deviations in pressure

$$\Delta P = 100(P_{calc} - P_{exp})/P_{exp} \tag{10}$$

where

$$P_{calc} = [RT/V(1 + B/V + C/V^2)] \tag{11}$$

Both the AAD and bias deviations in pressure are defined as in eqs 8 and 9, respectively.

Deviations in volume and pressure for each experimental point are illustrated in Figures 6 and 7 for the R32 + R236ea system and in Figures 8 and 9 for the R125 + R236ea system. The deviations for each isochore are presented in Table 10. Deviations are randomly distributed in both systems if they are plotted versus the reduced temperature. In general, the differences produced by eqs 7 and 10 are rather small, being within 0.02 dm^3/mol and

Table 10. Deviations in Pressure[a] and in Molar Volume[b] for the $P-V-T-x$ Data in the Superheated Vapor Region

	ΔP (%)		ΔV (dm^3 mol^{-1})			ΔP (%)		ΔV (dm^3 mol^{-1})	
sample	bias	AAD	bias	AAD	sample	bias	AAD	bias	AAD
	R32 + R236ea					R125 + R236ea			
1	−0.247	0.247	−0.013	0.013	1	−0.245	0.245	−0.011	0.011
2	−0.030	0.185	−0.001	0.008	2	−0.344	0.344	−0.010	0.010
3	0.041	0.106	0.001	0.003	3	−0.292	0.292	−0.006	0.006
4	1.308	2.692	0.021	0.040	4	−0.026	0.054	−0.001	0.003
5	2.913	3.520	0.029	0.035	5	0.082	0.102	0.003	0.004
6	0.733	0.847	0.009	0.011	6	−0.336	0.349	−0.012	0.012
7	−0.105	0.135	−0.005	0.006	7	−0.142	0.142	−0.004	0.004
8	0.103	0.111	0.004	0.005	8	0.023	0.060	0.000	0.001
9	−0.284	0.285	−0.006	0.006	9	0.133	0.133	0.001	0.001
10	−0.268	0.268	−0.041	0.041	10	−0.119	0.239	−0.002	0.005
average	0.156	0.535	−0.005	0.015	average	−0.137	0.190	−0.005	0.006

[a] Equation 31. [b] Equation 28.

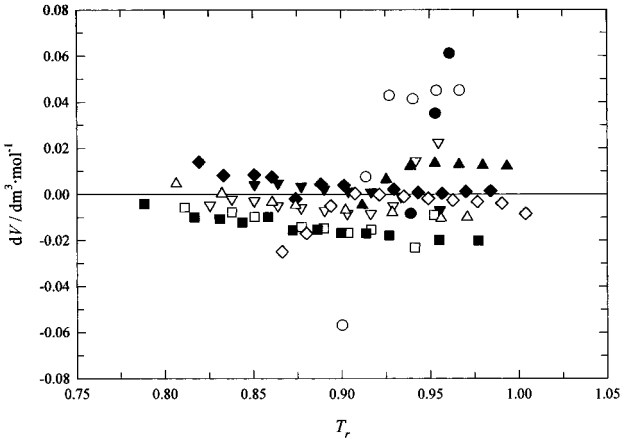

Figure 6. Deviations in molar volume versus reduced temperature for the R32 + R236ea system, for data in the superheated vapor region.

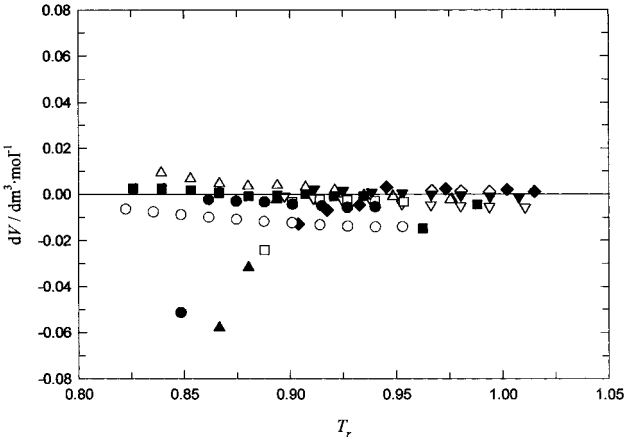

Figure 8. Deviations in molar volume versus reduced temperature for the R125 + R236ea system, for data in the superheated vapor region.

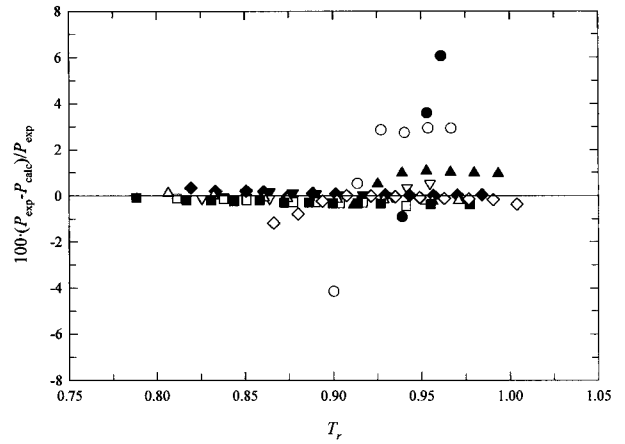

Figure 7. Deviations in pressure versus reduced temperature for the R32 + R236ea system, for data in the superheated vapor region.

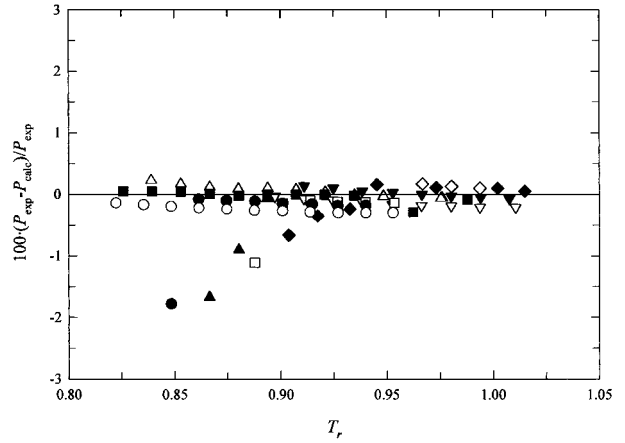

Figure 9. Deviations in pressure versus reduced temperature for the R125 + R236ea system for data in the superheated vapor region.

2% (disregarding a few points) in molar volume and pressure, respectively.

Conclusions

The random errors in the pressure representation are close to 1% in the representation of the superheated vapor pressures and have a 1−2% scatter in the VLE region, which makes them close to the values resulting from our error analysis, although in some cases, they are greater than expected. To date, for three of the four systems studied, we have found a small but systematic (positive) deviation on the order of 1−2% with respect to the VLE data in the literature determined by the direct (recirculation) method. The results obtained with the isochoric method are quite satisfactory. The advantage of this method is that, from the same run of experiments, we are able to cover wide temperature and pressure ranges and two regions of superheated vapor and within the VLE boundary. A disadvantage is presented by the difficulty in experimentally describing a complete VLE isotherm well. This could be a drawback especially for azeotropic mixtures.

Acknowledgment

This work has been supported by the European Union as part of the Joule Project within the IV Framework for RTD and by the Italian Ministero dell'Università e della Ricerca Scientifica e Tecnologica.

Literature Cited

(1) Di Nicola, G.; Polonara, F.; Stryjek, R. $P-V-T-x$ and VLE Properties of Pentafluoroethane (R125) + 1,1,1,3,3,3-Hexafluoroethane (R236fa) and 1,1,1,2-Tetrafluoroethane (R134a) + R236fa Systems Derived from Isochoric Measurements. *J. Chem. Eng. Data*. **2001**, *46* (2), 359.

(2) Di Nicola, G.; Giuliani, G.; Passerini, G.; Polonara, F.; Stryjek, R. Vapor−liquid−equilibrium (VLE) properties of R-32 + R-134a system derived from isochoric method. *Fluid Phase Equilib*. **1998**, *153*, 143−165.

(3) Di Nicola, G.; Giuliani, G. Vapor Pressure and $P-V-T$ Measurements for 1,1,1,2,3,3-Hexafluoropropane (R-236ea). *J. Chem. Eng. Data* **2000**, *45* (6), 1075−1079.

(4) Bobbo, S.; Fedele, L.; Scattolini, M.; Camporese, R. Vapor + liquid equilibrium measurements and correlationof the refrigerant mixtures difluoromethane (HFC-32) + and pentafluoroethane (HFC-125) + 1,1,1,2,3,3-hexafluoropropane (HFC-236ea) at 288.6, 303.2 and 318.3 K. *Int. J. Thermophys*. **2000**, *21*, 781−791.

(5) Giuliani, G.; Kumar, S.; Polonara, F. A constant volume apparatus for vapour pressure and gas phase $P-v-T$ measurements: validation with data for R22 and R134a. *Fluid Phase Equilib*. **1995**, *109*, 265−279.

(6) De Santis, R.; Gironi, F.; Marrelli, L. Vapor−liquid equilibrium from a hard-sphere equation of state. *Ind. Eng. Chem. Fundam*. **1976**, *15*, 183−189.

(7) Huber, M.; Gallagher, J.; McLinden, M. O.; Morrison, G. *NIST Thermodynamic Properties of Refrigerants and Refrigerants Mixtures Database (REFPROP)*, Version 5.0; Thermophysics Division, National Institute of Standards and Technology: Gaithersburg, MD, 1996.

(8) Reid, R. C.; Prausnitz, J. M.; Poling, B. E. *The Properties of Gases & Liquids*; McGraw-Hill: New York, 1987.

(9) Tsonopoulos, C. An empirical correlation of second virial coefficients. *AIChE J*. **1974**, *20*, 263−272.

(10) Tsonopoulos, C. An empirical correlation of second virial coefficients. *AIChE J*. **1975**, *21*, 827−829.

(11) Orbey, H.; Vera, J. H. Correlation for the third virial coefficient using T_c, P_c and ω as parameters. *AIChE J*. **1983**, *29*, 107−113.

Received for review August 8, 2000. Accepted December 4, 2000.

JE000260W